Optical monitoring of oxygen tension in cortical microvessels with confocal microscopy

Mohammad A. Yaseen[1], Vivek J. Srinivasan[1], Sava Sakadžić[1], Weicheng Wu[1], Svetlana Ruvinskaya[1], Sergei A. Vinogradov[2], and David A. Boas[1*]

[1]Photon Migration Imaging Laboratory, MGH/MIT/HMS Athinuola A. Martinos Center for Biomedical Imaging, Department of Radiology, Massachusetts General Hospital/Harvard Medical School,Building 149Room 2301,13th Street, Charlestown, MA 02129, USA

[2]Department of Biochemistry and Biophysics, University of Pennsylvania, 3700 Hamilton Walk, Philadelphia, PA 19104, USA

**dboas@nmr.mgh.harvard.edu*

Abstract: Evaluating cerebral oxygenation is of critical importance for the understanding of brain function and several neuropathologies. Although several techniques exist for measuring cerebral oxygenation *in vivo*, the most widely accepted techniques offer limited spatial resolution. We have developed a confocal imaging system for minimally invasive measurement of oxygen tension (pO_2) in cerebral microvessels with high spatial and temporal resolution. The system relies on the phosphorescence quenching method using exogenous porphyrin-based dendritic oxygen probes. Here we present high-resolution phosphorescence images of cortical microvasculature and temporal pO_2 profiles from multiple locations in response to varied fraction of inspired oxygen and functional activation.

©2009 Optical Society of America

OCIS codes: (180.1790) Confocal microscopy; (170.1470) Blood or tissue constituent monitoring; (170.3650) Lifetime-based sensing.

References and links

1. R. G. Shulman, F. Hyder, and D. L. Rothman, "Biophysical basis of brain activity: implications for neuroimaging," Q. Rev. Biophys. **35**(3), 287–325 (2002).
2. P. B. Jones, H. K. Shin, D. A. Boas, B. T. Hyman, M. A. Moskowitz, C. Ayata, and A. K. Dunn, "Simultaneous multispectral reflectance imaging and laser speckle flowmetry of cerebral blood flow and oxygen metabolism in focal cerebral ischemia," J. Biomed. Opt. **13**(4), 044007 (2008).
3. K. Nagata, M. Sato, Y. Satoh, Y. Watahiki, Y. Kondoh, M. Sugawara, G. Box, D. Wright, S. Leung, H. Yuya, and E. Shimosegawa, "Hemodynamic aspects of Alzheimer's Disease," Ann. N. Y. Acad. Sci. **977**(1), 391–402 (2002).
4. H. M. Swartz, "Measuring real levels of oxygen *in vivo*: opportunities and challenges," Biochem. Soc. Trans. **30**(2), 248–252 (2002).
5. J. L. Tatum, G. J. Kelloff, R. J. Gillies, J. M. Arbeit, J. M. Brown, K. S. C. Chao, J. D. Chapman, W. C. Eckelman, A. W. Fyles, A. J. Giaccia, R. P. Hill, C. J. Koch, M. C. Krishna, K. A. Krohn, J. S. Lewis, R. P. Mason, G. Melillo, A. R. Padhani, G. Powis, J. G. Rajendran, R. Reba, S. P. Robinson, G. L. Semenza, H. M. Swartz, P. Vaupel, D. Yang, B. Croft, J. Hoffman, G. Liu, H. Stone, and D. Sullivan, "Hypoxia: Importance in tumor biology, noninvasive measurement by imaging, and value of its measurement in the management of cancer therapy," Int. J. Radiat. Biol. **82**(10), 699–757 (2006).
6. F. Hyder, "Dynamic Imaging of Brain Function," in *Dynamic Brain Imaging: Multi-Modal Methods and In Vivo Applications*, F. Hyder, ed. (Humana Press, Totowa, NJ, 2009), pp. 3–21.
7. I. Kida, and F. Hyder, "Physiology of Functional Magnetic Resonance Imaging," in *Magnetic Resonance Imaging: Methods and Biologic Applications*, P. V. Prasad, ed. (Humana Press Inc., Totowa, NJ, 2006).
8. D. S. Vikram, J. L. Zweier, and P. Kuppusamy, "Methods for Noninvasive Imaging of Tissue Hypoxia," Antioxid. Redox Signal. **9**(10), 1745–1756 (2007).
9. W. L. Rumsey, J. M. Vanderkooi, and D. F. Wilson, "Imaging of Phosphorescence: A Novel Method for Measuring Oxygen Distribution in Perfused Tissue," Science **241**(4873), 1649–1651 (1988).
10. S. A. Vinogradov, L.-W. Lo, and D. F. Wilson, "Dendritic Polyglutamic Porphyrins: Probing Porphyrin Protection by Oxygen-Dependent Quenching of Phosphorescence," Chem. Eur. J. **5**(4), 1338–1347 (1999).
11. I. Dunphy, S. A. Vinogradov, and D. F. Wilson, "Oxyphor R2 and G2: phosphors for measuring oxygen by oxygen-dependent quenching of phosphorescence," Anal. Biochem. **310**(2), 191–198 (2002).
12. A. Y. Lebedev, A. V. Cheprakov, S. Sakadžić, D. A. Boas, D. F. Wilson, and S. A. Vinogradov, "Dendritic Phosphorescent Probes for Oxygen Imaging in Biological Systems," ACS Applied Materials & Interfaces **1**(6), 1292–1304 (2009).

#116684 - $15.00 USD Received 4 Sep 2009; revised 18 Oct 2009; accepted 22 Oct 2009; published 23 Nov 2009

13. I. P. Torres Filho, and M. Intaglietta, "Microvessel PO_2 measurements by phosphorescence decay method," Am. J. Physiol. **265**(4 Pt 2), H1434–H1438 (1993).
14. R. D. Shonat, D. F. Wilson, C. E. Riva, and M. Pawlowski, "Oxygen distribution in the retinal and choroidal vessels of the cat as measured by a new phosphorescence imaging method," Appl. Opt. **31**(19), 3711–3718 (1992).
15. M. Intaglietta, P. C. Johnson, and R. M. Winslow, "Microvascular and tissue oxygen distribution," Cardiovasc. Res. **32**(4), 632–643 (1996).
16. E. G. Mik, T. Johannes, and C. Ince, "Monitoring of renal venous PO_2 and kidney oxygen consumption in rats by a near-infrared phosphorescence lifetime technique," Am. J. Physiol. Renal Physiol. **294**(3), F676–F681 (2008).
17. R. L. Plant, and D. H. Burns, "Quantitative, Depth-Resolved Imaging of Oxygen Concentration by Phosphorescence Lifetime Measurement," Appl. Spectrosc. **47**(10), 1594–1599 (1993).
18. I. Filho, M. Leunig, F. Yuan, M. Intaglietta, and R. K. Jain, "Noninvasive measurement of microvascular and interstitial oxygen profiles in a human tumor in SCID mice," Proc. Natl. Acad. Sci. U.S.A. **91**(6), 2081–2085 (1994).
19. I. P. Torres Filho, H. Kerger, and M. Intaglietta, "pO_2 Measurements in Arteriolar Networks," Microvasc. Res. **51**(2), 202–212 (1996).
20. A. G. Tsai, B. Friesenecker, M. C. Mazzoni, H. Kerger, D. G. Buerk, P. C. Johnson, and M. Intaglietta, "Microvascular and tissue oxygen gradients in the rat mesentery," Proc. Natl. Acad. Sci. U.S.A. **95**(12), 6590–6595 (1997).
21. D. F. Wilson, S. A. Vinogradov, P. Grosul, M. N. Vaccarezza, A. Kuroki, and J. Bennett, "Oxygen distribution and vascular injury in the mouse eye measured by phosphorescence-lifetime imaging," Appl. Opt. **44**(25), 5239–5248 (2005).
22. A. S. Golub, and R. N. Pittman, "PO2 measurements in the microcirculation using phosphorescence quenching microscopy at high magnification," Am. J. Physiol. Heart Circ. Physiol. **294**(6), 2905–2916 (2008).
23. A. S. Golub, M. C. Barker, and R. N. Pittman, "Microvascular oxygen tension in the rat mesentery," Am. J. Physiol. Heart Circ. Physiol. **294**(1), H21–H28 (2007).
24. O. S. Finikova, A. Y. Lebedev, A. Aprelev, T. Troxler, F. Gao, C. Garnacho, S. Muro, R. M. Hochstrasser, and S. A. Vinogradov, "Oxygen Microscopy by Two-Photon-Excited Phosphorescence," ChemPhysChem **9**(12), 1673–1679 (2008).
25. A. D. Estrada, A. Ponticorvo, T. N. Ford, and A. K. Dunn, "Microvascular oxygen quantification using two-photon microscopy," Opt. Lett. **33**(10), 1038–1040 (2008).
26. E. M. C. Hillman, A. Devor, M. B. Bouchard, A. K. Dunn, G. W. Krauss, J. Skoch, B. J. Bacskai, A. M. Dale, and D. A. Boas, "Depth-resolved optical imaging and microscopy of vascular compartment dynamics during somatosensory stimulation," Neuroimage **35**(1), 89–104 (2007).
27. S. Sakadžić, S. Yuan, E. Dilekoz, S. Ruvinskaya, S. A. Vinogradov, C. Ayata, and D. A. Boas, "Simultaneous imaging of cerebral partial pressure of oxygen and blood flow during functional activation and cortical spreading depression," Appl. Opt. **48**(10), D169–D177 (2009).
28. E. P. Vovenko, "Distribution of oxygen tension on the surface of arterioles, capillaries, and venules of brain cortex and in tissue in normoxia: an experimental study on rats," Pfluegers Arch. Eur. J. Physiol. **437**(4), 617–623 (1999).
29. K. Masamoto, T. Kurachi, N. Takizawa, H. Kobayashi, and K. Tanishita, "Successive depth variations in microvascular distribution of rat somatosensory cortex," Brain Res. **995**(1), 66–75 (2004).
30. R. V. Harrison, N. Harel, J. Panesar, and R. J. Mount, "Blood Capillary Distribution Correlates with Hemodynamic-based Functional Imaging in Cerebral Cortex," Cereb. Cortex (Cary) **12**(3), 225–233 (2002).
31. S. A. Vinogradov, L.-W. Lo, W. T. Jenkins, S. M. Evans, C. Koch, and D. F. Wilson, "Noninvasive Imaging of the Distribution in Oxygen in Tissue In Vivo Using Near-Infrared Phosphors," Biophys. J. **70**(4), 1609–1617 (1996).
32. F. Reina-De La Torre, A. Rodriguez-Baeza, and J. Sahuquillo-Barris, "Morphological Characteristics and Distribution Pattern of the Arterial Vessels in Human Cerebral Cortex: A Scanning Electron Microscope Study," Anat. Rec. **251**(1), 87–96 (1998).

1. Introduction

In brain tissue, assessing parameters to quantify oxidative metabolism is crucial for gaining insight into brain function [1]. Evaluating factors such as oxygen extraction fraction (OEF) and cerebral metabolic rate of oxygen ($CMRO_2$) are also important to understand and develop treatments for neuropathologies, including stroke and Alzheimer's disease [2, 3].

A number of techniques exist to evaluate oxygen metabolism *in vivo* [4–6], including blood-oxygen level dependent magnetic resonance imaging (BOLD-MRI), positron emission tomography (PET), polarographic electrodes, and near infrared spectroscopy (NIRS). In particular, BOLD-MRI, PET, and NIRS are noninvasive and are utilized widely in clinical research. Each technique, however, has associated limitations. In addition to requiring expensive instrumentation, BOLD-MRI provides an indirect measure of oxygen consumption through measurements of deoxy-hemoglobin concentration. PET yields measurements of OEF by monitoring the circulation of radionucleotides such as of ^{15}O. Each of these

#116684 - $15.00 USD Received 4 Sep 2009; revised 18 Oct 2009; accepted 22 Oct 2009; published 23 Nov 2009
(C) 2009 OSA

techniques also has limited spatial resolution, ranging from hundreds of micrometers to centimeters [7, 8]. Polarographic electrodes are capable of fast, direct measurements of oxygen partial pressure with spatial resolution dependent on the electrode diameter (ranging from 10 to 1000 micrometers) but electrodes are invasive, susceptible to noise, and measurements are confined to discrete locations [4].

We have developed a confocal optical imaging system capable of measuring oxygen partial pressure (pO_2) in microvessels with high spatial resolution. The performance of the system is demonstrated by minimally-invasive observations of pO_2 in cortical vasculature of rats.

The system utilizes phosphorescence lifetime imaging [9] in combination with confocal microscopy using O_2-sensitive phosphorescent probes [10–12] to yield absolute pO_2 measurements with high spatial and temporal resolution. Dissolved O_2 molecules dynamically quench the phosphorescence of Pd porphyrin-based dendritic oxygen probes, such as Oxyphor R2 [10, 11]. The measured phosphorescence lifetime is used to calculate pO_2. The phosphorescence lifetime technique, in its both time- and frequency-domain variants, has been utilized extensively to measure pO_2 *in vivo* [9, 13–16]. Several examples of microscopic measurements of phosphorescence have been reported [17–23], More recent reports focused on multiphoton excitation [24, 25]. In particular, Estrada et al demonstrated depth-resolved intravascular pO_2-quantification in cortical microvasculature using multiphoton microscopy and Oxyphor R2. Our confocal system allows us to probe pO_2 in vessels with high transverse and axial resolution, avoiding phosphorescence signal contamination from neighboring or underlying vessels with different pO_2. Additionally, by limiting the area of illuminated tissue for a measurement, both multiphoton and confocal microscopy reduce the prospect of measurement errors introduced by photoconsumptive effects of the dye [22]. Although light-scattering by brain tissue limits confocal measurements to the most superficial layer of the cortex, the single-photon excitation efficiency of Oxyphor R2 is considerably higher than its 2-photon efficiency. This allows for faster data collection, avoiding excessively long data averaging, enabling us to perform pO_2 measurement at multiple locations with good temporal resolution. To our knowledge, our system is the first to allow nearly-simultaneous dynamic monitoring of pO_2 at multiple locations.

We continuously monitored changes in pO_2 at numerous locations while changing the fraction of inspired oxygen (FiO_2) and during functional brain stimulation. pO_2 profiles reveal considerable heterogeneity within distances that cannot be resolved with conventional O_2 measurement techniques. These results represent our initial steps toward quantification of the cerebral metabolic rate of O_2 ($CMRO_2$) with high spatial resolution.

2. Materials and methods

2.1 Animal preparation

Animals were prepared under a protocol approved by the Subcommittee on Research Animal Care at Massachusetts General Hospital. Using a procedure described previously [26], cortical vessels of Sprague Dawley rats (250 – 300g) were imaged through a sealed cranial window over the somatosensory cortex. Briefly, while under isoflurane anesthesia, a tracheotomy and cannulation of the femoral artery and vein were performed. After fixing the head in a stereotactic frame, the scalp was retracted, and 3 x 3 mm sections of the skull and dura mater were removed over the coronal suture. The somatosensory cortex was exposed for functional activation experiments, while for the varied FiO_2 measurements, the skull and dura mater were removed over a region along the coronal suture closer to the bregma. After brain exposure, a glass cover slip window was then applied using agarose gel and dental acrylic cement. For the duration of the experiments, isoflurane inhalation was replaced with a continuous infusion of α-chloralose. Arterial blood pressure, heart rate, body temperature, and blood gas measurements were monitored continuously throughout the experiments. Using a ventilator, the animals' breathing was controlled mechanically with gas fractions adjusted to yield suitable blood gas measurements.

#116684 - $15.00 USD Received 4 Sep 2009; revised 18 Oct 2009; accepted 22 Oct 2009; published 23 Nov 2009
(C) 2009 OSA

2.2 Phosphorescence lifetime microscopy

Confocal imaging was used to evaluate pO_2 by measuring phosphorescence of exogenous, O_2-sensitive dyes confined to the vasculature. A commerically available probe Oxyphor R2 (Oxygen Enterprises, Philadelphia, PA) was utilized in these studies.Oxyphor R2 is highly soluble in water, and its phosphorescence lifetimes range from 20 to 620 μs in the physiological pO_2 range (159-0 mm Hg), provided the probe is bound to albumin [11]. After dissolving it in saline, Oxyphor R2 was administered as a bolus injection through the femoral vein at a concentration of 6.7 mg/kg body weight (approximately 40 μM concentration in blood).

The confocal portion of our custom-designed multi-modal imaging system is depicted in Fig. 1. An electro-optical modulator (ConOptics, Danbury, CT) temporally gates the output of a CW diode laser (λ = 532 nm, B&W Tek) with an extinction ratio of approximately 200 at λ = 532 nm. The excitation beam passes through several conditioning optics, including a beam expander with pinhole spatial filter, polarizer, shutter, dichroic mirror, scan lens, and tube lens. Galvanometric scanners (xy, Cambridge Technology, Inc. Lexington, MA) guide the excitation beam to selected locations on the object. Light is focused onto the sample using a 20x-magnification objective lens (XLumPlan FL, Olympus, NA = 0.95). The average excitation power on the sample was 10 mW. The emitted phosphorescence was de-scanned and collected using an avalanche photodiode photon counting module (APD, SPCM-AQRH-10, Perkin Elmer, Waltham, MA). The APD's active area (180 μm diameter) functions as the second pinhole for confocal imaging. By focusing the emission light to a size smaller than the pinhole size, signal to noise ratio was increased at the cost of slightly reducing spatial resolution of the system, yielding calculated lateral and axial resolutions of 1 μm and 2.4 μm, respectively.

The system is controlled using two computers running custom-designed software written in LabView (National Instruments, Austin,TX). The first computer (PC1) contains a data acquisition board with analog inputs and digital outputs to control and synchronize the EOM and scanner mirrors. The software on PC1 allows for adjustable temporal gating of the excitation beam, and selection of intravascular points at which pO_2 values can be measured. The second computer (PC2) collects photon counting data from the APD with a high speed DIO card (PCIe-7537, National Instruments, Austin TX), performs subsequent image processing.

#116684 - $15.00 USD Received 4 Sep 2009; revised 18 Oct 2009; accepted 22 Oct 2009; published 23 Nov 2009
(C) 2009 OSA

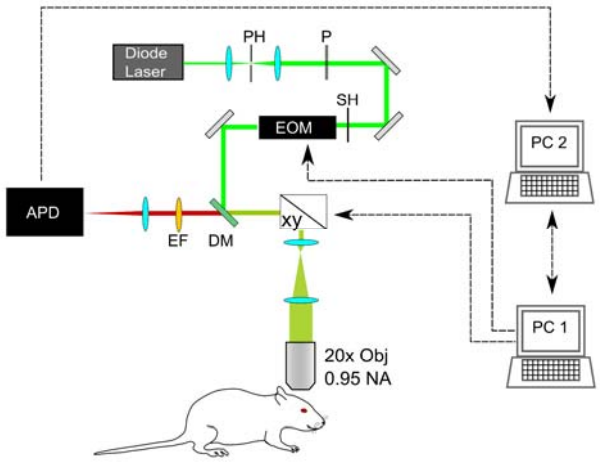

Fig. 1. Schematic for confocal lifetime imaging system. Excitation light is provided by a diode laser λ=532 nm, which is spatially filtered with a pinhole (PH), polarized with a Glan laser calcite polarizer (P), and temporally gated with a shutter (SH) and electro-optical modulator (EOM). Excitation light is focused onto the cranial window using a 20x magnification objective (OBJ) with 0.95 numerical aperture. Focused light is directed to points of interest using galvanometric scanners (xy). Emitted phosphorescence light is detected using the same objective. It is spectrally separated from excitation light using a dichroic mirror (DM) and emission filter (EM) and detected with an avalanche photodiode (APD). The system is controlled by 2 computers (PC1, PC2) running custom-designed software.

Imaging is performed in two steps. Initially, survey scan phosphorescence images are generated by scanning over the field of view and summing the photon counts at each pixel. For these images, the excitation duration (the time during which the EOM transmits the maximal amount of excitation light, shaded region in Fig. 2.(b)) and the phosphorescence detection time (i.e. the time during which the EOM blocked the excitation light) are both set to approximately 50 μs. These parameters were selected to minimize exposure of the tissue to the light and to expedite image acquisition while still yielding sufficient signal. It requires roughly 6 seconds to acquire a 250 x 250 pixel image. After generating the survey scan image of the entire field of view, points of interest are identified within the pial vessels for pO_2 measurement. Longer excitation duration and detection time (approximately 100 μs and 500 μs, respectively) are utilized when measuring pO_2 at selected points. These durations were selected to ensure saturation of the probe triplet state in the focal volume for maximal signal output and for collection of the adequate portion of the phosphorescence decay. At each point, this excitation and detection cycle is repeated approximately 50 times to increase the signal to noise ratio. Consequently, each pO_2 measurement for a given location requires between 30 and 50 ms, depending upon the number of cycles and the time required to position the galvanometer mirrors.

The phosphorescence quenching technique gives rise to reactive singlet oxygen molecules as a reaction by-product. Care must be taken to avoid photo-oxidative damage to the vasculature and tissue from excessive singlet oxygen. Exposure to ambient light was minimized by surrounding the entire system in a light-tight enclosure, and the laser exposure was limited using the shutter and EOM. Additionally, experimental parameters such as excitation intensity and duration, dye concentration, experiment duration, and pO_2 measuring intervals were selected to minimize photo-oxidative damage. During our experiments, survey scan phosphorescence images were obtained intermittently to check for dye extravasation, an indicator of photo-oxidative damage.

#116684 - $15.00 USD Received 4 Sep 2009; revised 18 Oct 2009; accepted 22 Oct 2009; published 23 Nov 2009
(C) 2009 OSA

All data are processed using software custom-written in C and MATLAB (Mathworks, Natick, MA). The APD module outputs a TTL pulse for each detected photon, which is collected with a high speed DIO card, operating at a 50 MHz sampling rate. The counts are binned into 10 μs-long bins. Using a nonlinear least squares fitting routine, the resulting data are fit with a single-exponential function:

$$I(t) = I_0 \exp\left(-\frac{t}{\tau}\right) + c \quad (1)$$

in which the first term represents the phosphorescence decay of Oxyphor R2 and the second term corresponds to background signal that results primarily from imperfect rejection of excitation light by the EOM. In most cases, magnitude of the baseline (c) was found to be much smaller than the amplitude of the phosphorescence decay (I_0). It should be mentioned that in spite of the fact that phosphorescence decays of R2, as well as all other albumin-bound probes, are non-single-exponential, we chose to apply single-exponential fitting in order to achieve lower noise in the estimated parameter τ. This necessitated use of an empirically constructed non-linear Stern-Volmer-like curve [27], in order to maintain accuracy of oxygen measurements. Non-single-exponentiality of the probe decay is a result of a multiple conformations of the R2-albumin complex as well as of the presence of unbound R2 at higher R2/albumin ratios. Higher concentration was required in our experiments in order to achieve optimal photon counts.

2.3 Variable FiO_2 experiments

We tested our system's ability to monitor pO_2 in vasculature by varying a rat's fraction of inspired oxygen (FiO_2). Gas fractions were adjusted to yield an initial pO_2 within 90-100 mmHg in the femoral artery, measured with a blood gas analyzer. At t = 30 s, the inspired gas fractions were adjusted to lower the FiO_2 from 21% to 14% for 10 minutes. Following this, the FiO_2 was increased to 60%. For the duration of the experiments, the shutter was opened every 5 seconds, and pO_2 values were measured at selected locations. Measurements were binned into 30-second intervals during post-processing.

2.4 Functional stimulation experiments

pO_2 levels were observed at selected points during functional brain stimulation. Current pulses (~2 mA amplitude, 300 μs duration) were delivered to the rat's forepaw at 3 Hz for 4s. Prior to the pO_2 measurement, the animals were initially imaged with optical intrinsic signal imaging (OISI) to determine the location, magnitude, and stability of the stimulus response following a procedure similar to that described by Hillman et al [26]. The cranial window was illuminated with 570 nm light, delivered with a fiber from a spectrally-filtered Hg:Xe lamp, and imaged with a CCD camera at 25 frames/sec. As λ = 570 nm is an isosbestic point for hemoglobin, an increase in blood volume would result in a local reduction of diffusely reflected intensity at the area of cortical activation. After the activation area was identified with OISI, pO_2 values were measured within this area with our confocal imaging system at selected locations of interest at 1-second intervals.

3. Results and discussion

Figure 2(a) displays a color-coded angiogram of pial vessels in the rat cortex, collected by integrating the R2 phosphorescence intensity at each pixel during a survey scan. Selected

#116684 - $15.00 USD Received 4 Sep 2009; revised 18 Oct 2009; accepted 22 Oct 2009; published 23 Nov 2009
(C) 2009 OSA

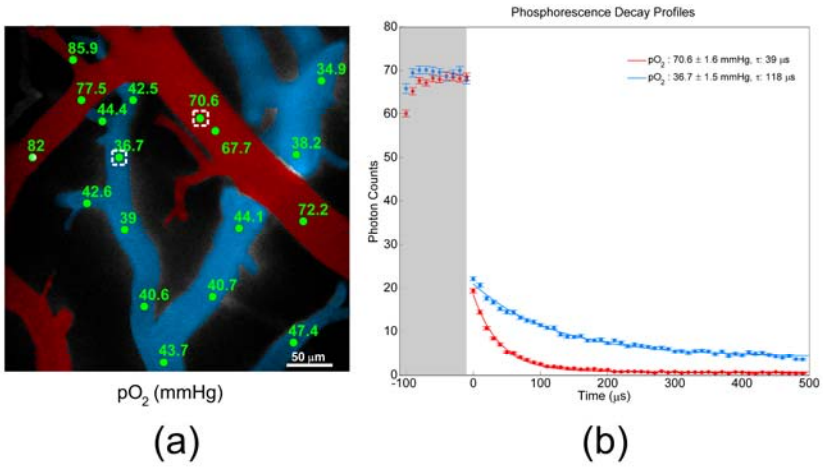

Fig. 2. (a) Color-coded angiogram of pial microvasculature from an exposed cranial window. Arterioles are indicated in red, and venules are blue. Measured pO_2 values (mmHg) at selected intravascular locations are indicated in green. (b) Phosphorescence decay profiles measured at points identified with white boxes in Fig. 2(a). Higher O_2 concentration in the arteriole causes more quenching of phosphorescence signal, and consequently a faster decay (red profile).

intravascular locations and corresponding pO_2 measurements during normoxia are identified in green, and representative excitation and decay profiles are provided in Fig. 2(b). The shaded region corresponds to the excitation interval, during which the EOM transmits the excitation light. In both arterioles and venules, saturation of the phosphorescence generally occurs within approximately 40 μs under normoxic conditions. Our measurements (76.0 ± 7.1 mmHg in arterioles, 41.2 ± 3.6 mmHg in venules) were found to agree well with reported measurements in similar-sized vessels during normoxia (78.7 ± 8.9 mmHg in arterioles, 40.1 ± 9.1 mmHg in venules) performed with a polarographic electrode [28]. Phosphorescence quenching is mitigated in the venules, where dissolved O_2 concentration is approximately half as high as in arterioles, leading to higher amounts of detected phosphorescence signal. pO_2 varies dramatically over approximately 400 x 400 μm^2.

Figure 3 shows pO_2 profiles at selected vessel locations as the rat's FiO_2 was altered from 21% to 14%, then to 60%. Again, the pO_2 measurements during normoxia (69.4 ± 7.9 mmHg in arterioles, 43.0 ± 3.5 mmHg in venules) agreed well with previously-reported results. During the first few minutes at lowered FiO_2, the surplus O_2 in the bloodstream is depleted to sustain metabolic demand. pO_2 levels initially decrease during the first several minutes, after which pO_2 maintains a lower steady state value. The phenomenon appeared invariant of location within the brain or vessel type. During the induced hypoxic period, arterioles experienced a mean reduction of 15.7 ± 8.0 mmHg, while the average reduction in venules was 12.3 ± 1.9 mmHg. In both arteries and veins, comparable time periods were needed to reach new steady state hypoxic pO_2 values: 185.0 ±12.2 s in arteries and 195.0 ±56.1 s in veins.

Upon increasing the FiO_2 from 14% to 60%, pO_2 recovered to initial values within one minute and greatly exceeded baseline values. The pO_2 response to increased FiO_2 was found to vary between arterioles and venules. An increase of 52.9 ± 22.1 mmHg in arterioles and 14.1 ± 9.5 mmHg in venules from normoxic values during hyperoxia was observed. Upon inducing a higher FiO_2, pO_2 changes occurred more rapidly than during the hypoxic period. pO_2 values reached their peak values after 135.0 ± 16.4 s in arteries and after 130.0 ± 15.5 s in veins.

#116684 - $15.00 USD Received 4 Sep 2009; revised 18 Oct 2009; accepted 22 Oct 2009; published 23 Nov 2009
(C) 2009 OSA

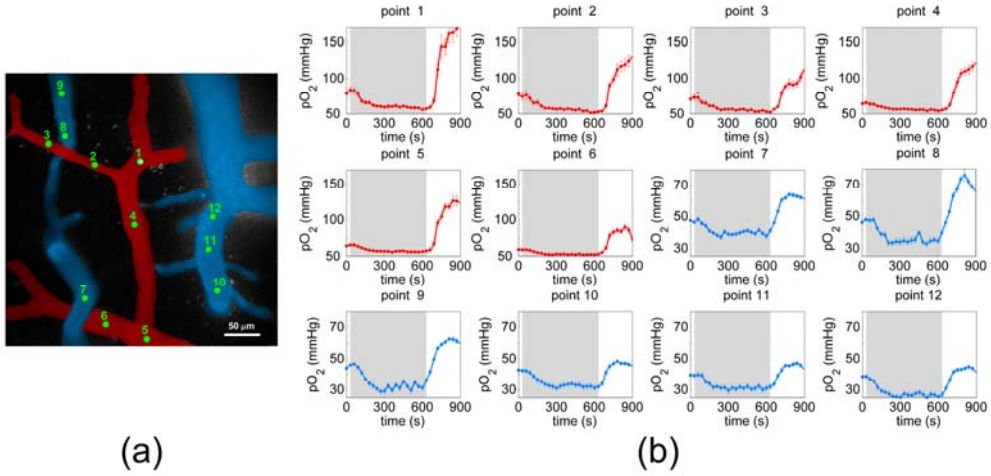

Fig. 3. (a) Color-coded angiogram of cortical pial microvasculature. Green points identify intravascular locations where pO_2 measurements were taken, and (b) corresponding temporal profiles of pO_2 during measured while altering FiO_2. The grey segments denote the 10 minute period during which FiO_2 was lowered to 14%. Following this 10-minute duration, FiO_2 was immediately increased up to 60%.

Figure 4(a) displays a cranial window prepared for functional stimulation experiments, imaged with a CCD camera and 570 nm diffuse light. The area imaged during confocal pO_2 experiments is indicated by the overlaid angiogram. The shaded green region corresponds to the region that experienced maximal increase in hemoglobin concentration during forepaw stimulation, as determined by OISI. Figure 4(c) depicts temporal pO_2 profiles from locations identified in Fig. 4(b). The grey regions in Fig. 4(c) denote a 4-second interval during which an electrical stimulus train was delivered to the animal's forepaw. The profiles show the averaged measurements of 14 stimulus trials, with each stimulus delivered 30 seconds apart. Mean baseline pO_2 values for arterioles and venules were slightly higher than previously reported at 88.3 ± 13.0 mmHg and 54.9 ± 2.2 mmHg, respectively [28]. The profiles display considerable heterogeneity, with only select intravascular locations demonstrating the distinctive rise in pO_2 characteristic of a brief forepaw stimulus [29]. Only select vessels in the field of view supply and drain blood from the activated area. A pO_2 increase of approximately 10 mmHg was observed in the arterioles that feed the activated area (points 10 and 11), while an increase of 2 mmHg was seen in the draining venules (points 1, 4, and 5). The pO_2 changes in arterioles are comparable to the previously-reported Clark electrode measurements of tissue pO_2 during functional stimulation [27, 30]. A somewhat smaller increase seen in venules is comparable to the measurements by phosphorescence using Oxyphor R2 and either a local 2 mm optical fiber probe or widefield imaging CCD-based imaging setup [27, 31]. As seen by points 1-7, the response varies greatly between neighboring venules that drain into the same vein, suggesting that merging venules less than 100 μm apart on the surface drain from functionally distinct regions within the cortex. This observation is consistent with previous reports which evaluated the cortical vasculature using corrosion casts [29, 30]. Branching arterioles and merging venules run parallel to the surface for large distances before diving into functionally distinct regions. Additionally, the underlying microvessels supplied and drained by the surface vessels are also quite tortuous, extending in various directions throughout the cortical layers.

#116684 - $15.00 USD Received 4 Sep 2009; revised 18 Oct 2009; accepted 22 Oct 2009; published 23 Nov 2009
(C) 2009 OSA

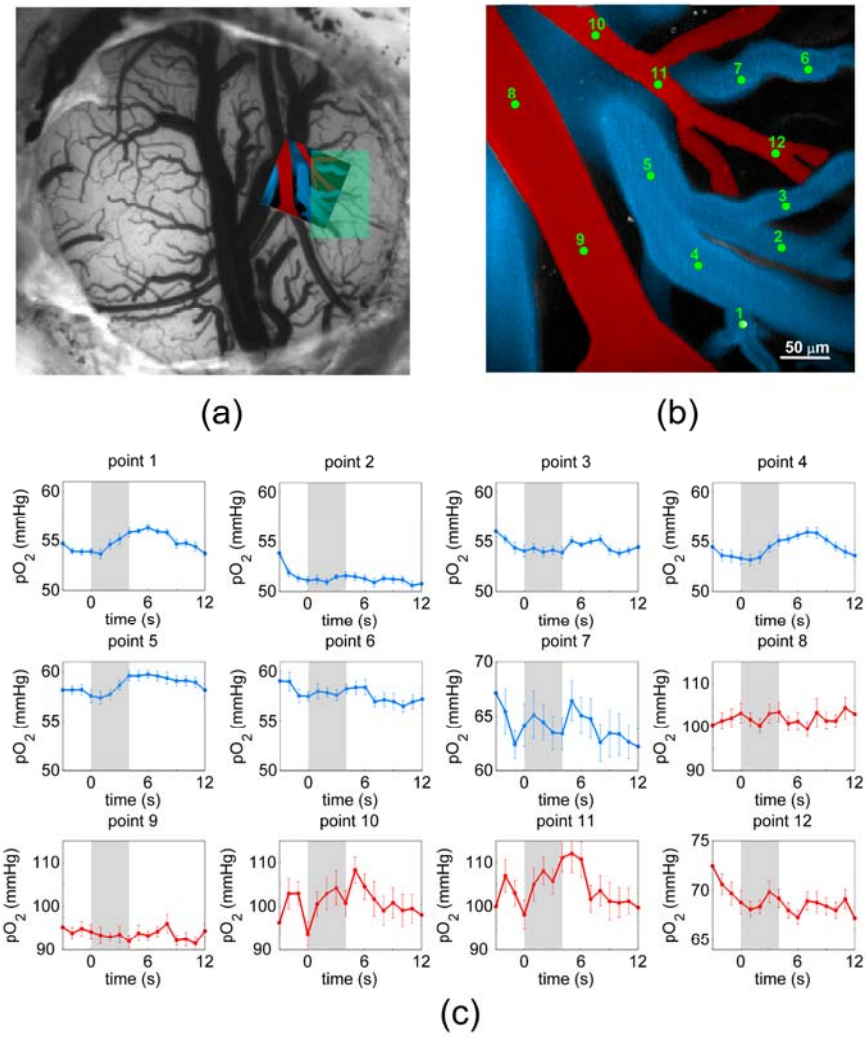

Fig. 4. (a) CCD image of cranial window with confocal angiogram overlaid and region of functional activation identified in green (b) Color-coded angiogram of microvessels in rat somatosensory cortex, with identified locations for pO_2 measurement. (c) Temporal profiles of pO_2 during functional stimulation.

Over the course of our experiments, we monitored physiological signals from the animals, including arterial blood pressure, heart rate, body temperature, and arterial blood gas levels. We found that intravenous administration of R2 had no effect on the monitored physiological signals. Our observations are consistent with other reported experiments in which no evidence of toxicity was observed from Pd-porphyrin dyes up to 10 days post administration [31].

Light-scattering by brain tissue limits our confocal pO_2 measurements to pial vessels on the cortical surface. Consequently, our system can currently probe only arterioles and venules that either run parallel to the cortical surface or dive downward to supply or drain the capillary network located hundreds of microns beneath the cortical surface [30, 32]. The use of deeper-penetrating multiphoton microscopy allows for pO_2 measurements within diving arterioles and the capillary network, the primary sites of O_2 delivery to cortical tissue [28]. Estrada et al has reported multiphoton measurements using Oxyphor R2, allowing for depth-resolved intravascular pO_2-quantification in the rat cortex [25]. By measuring pO_2 within a bifurcating vessel with an occluded branch, they demonstrated that oxygen is still transported

#116684 - $15.00 USD Received 4 Sep 2009; revised 18 Oct 2009; accepted 22 Oct 2009; published 23 Nov 2009
(C) 2009 OSA

by plasma in vessels downstream from an occlusion where no erythrocytes are present. They compensated for Oxyphor R2's low 2-photon cross section by administering 10 times more than the amount used in our experiments. In addition, the Oxyphor R2 was administered as a mixture with dextran-conjugated fluorescein to generate suitable image contrast. Each pO_2 measurement required collection of 2000 decays at each point to yield a reliable pO_2 value, thus limiting the temporal resolution of the method. Combining lifetime-based pO_2-monitoring with multiphoton excitation offers considerable potential for future cerebral oxygenation investigations. The limitations presented by Oxyphor R2's low 2-photon cross-section, however, encourage the use of new two-photon excitable phosphorescent probes such as PtP-C343 [24].

4. Conclusion

Our phosphorescence lifetime microscopy system is useful for minimally invasive measurement of oxygen partial pressure in cortical vessels with high spatial and temporal resolution. The results show that pO_2 varies considerably within distances that currently cannot be resolved using conventional O_2-monitoring techniques and illustrate the need for pO_2 measurement techniques at multiple locations with high spatial and temporal resolution.

Our system demonstrates potential for characterizing cerebral pO_2 under several different physiological and pathophysiological conditions. When coupled with simultaneous blood flow measurements, the system can yield high-resolution quantification of $CMRO_2$ and provide a better understanding of metabolic dynamics under various neuropathologies.

Acknowledgements

This work was supported by NIH R01-NS057476, P50-NS010828, K99NS067050, and P01-NS055104.

#116684 - $15.00 USD Received 4 Sep 2009; revised 18 Oct 2009; accepted 22 Oct 2009; published 23 Nov 2009
(C) 2009 OSA